Title

Distortion, Tether, and Entropy Effects on Transannular Diels–Alder Cycloaddition Reactions of 10–18-Membered Rings

Journal

The Journal of Organic Chemistry, 80(21)

ISSN

0022-3263

Authors

He, Cyndi Qixin
Chen, Tiffany Q
Patel, Ashay
et al.

Publication Date

2015-11-06

DOI

10.1021/acs.joc.5b02288

Peer reviewed

JOC The Journal of Organic Chemistry

Article

pubs.acs.org/joc

Distortion, Tether, and Entropy Effects on Transannular Diels–Alder Cycloaddition Reactions of 10–18-Membered Rings

Cyndi Qixin He,[†] Tiffany Q. Chen,[†] Ashay Patel,[†] Sedef Karabiyikoglu,[†] Craig A. Merlic,*[,†] and K. N. Houk*[,†,‡]

[†]Department of Chemistry and Biochemistry and [‡]Department of Chemical and Biochemical Engineering, University of California, Los Angeles, California 90095, United States

Supporting Information

ABSTRACT: Density functional theory calculations were performed on a set of 13 transannular Diels–Alder (TADA) reactions with 10–18-membered rings. The results were compared with those for bimolecular and intramolecular Diels–Alder reactions in order to investigate the controlling factors of the high TADA reactivities. The effects of tether length, heteroatoms, and alkynyl dienophiles on reactivity were analyzed. We found a correlation between tether length and reactivity, specifically with 12-membered macrocycles undergoing cycloaddition most readily. Furthermore, modifying 12-membered macrocycles by heteroatom substitution and utilizing alkynyl dienophiles enhances the reaction rates up to 10^5-fold.

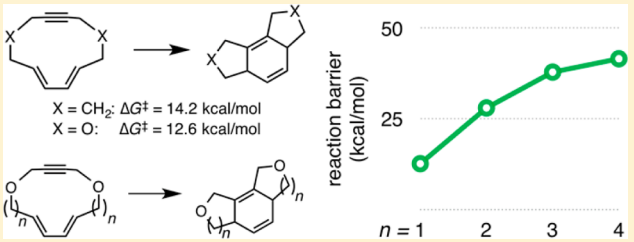

INTRODUCTION

The Diels–Alder reaction has been widely employed in organic synthesis to construct six-membered carbocyclic compounds since its discovery in 1928.[1] The prototypical Diels–Alder reaction of butadiene and ethene is very slow, but it is accelerated by appropriate substitution to confer nucleophilic and electrophilic character on the diene and dienophile, or vice versa.[2−4] Intramolecular Diels–Alder reactions, which have been well studied both experimentally and computationally, exhibit higher reaction rates due to the minimization of entropic penalties by linking the reacting moieties in a single molecule.[5,6]

Transannular Diels–Alder (TADA) reactions are particularly interesting, because the macrocyclic reactants are often found to undergo Diels–Alder reactions rapidly under exceptionally mild conditions even below room temperature.[7] Furthermore, they are effective in giving rise to tricyclic molecules with predictable stereochemistry at the ring junctions, which can serve as the structural backbone for a wide range of natural products.[8]

The greatest challenge for successful transannular reactions is to synthesize the requisite macrocycles efficiently. Deslongchamps and co-workers were the first to report methods to prepare macrocyclic substrates in the early 1990s, utilizing a Pd(0) catalyst to prepare 10–14-membered rings.[9−11] In 2013, Merlic and co-workers developed a new method to synthesize a range of cyclic trienes and dienynes by Pd(II)-catalyzed macrocyclizations (Scheme 1).[12,13] This method enables the syntheses of a broad range of macrocycles that contain diene and dienophile joined by two tethers.

Scheme 2 shows six TADA reactions of macrocycles reported earlier.[12] The macrocycles in eqs 1–3a are 12-membered rings

Scheme 1. Methodology Developed by Merlic and Co-Workers for Macrocyclizations[12,13]

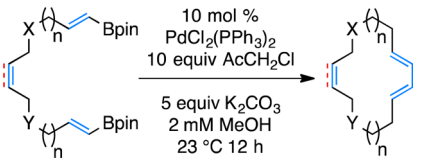

with *cis*-alkenyl, *trans*-alkenyl, and alkynyl dienophiles; the macrocycle in eq 3b also contains an alkynyl dienophile, and the oxygen atoms are replaced by nitrogen atoms in the tethers.

None of the 12-membered macrocycles were isolable and instead directly gave the tricyclic cycloaddition products in high yields (Scheme 2 eqs 1–3). The 14-membered substrates such as macrocycles **7** and **9** in eqs 4 and 5 were less reactive and could be isolated and characterized. The 14-membered hydrocarbon macrocycle underwent a TADA reaction readily to form the corresponding [6,6,6]-fused tricyclic product. The TADA reaction was not observed to give the [5,6,7]-fused tricyclic product with unsymmetrical macrocycle **9** (eq 5). Macrocycles **1** and **7** gave *endo* and *exo* isomers, respectively.

More recent results on a series of dioxa macrocycles featuring a diene and an alkyne dienophile showed that the length of the oxygen-containing tethers dramatically influences TADA reactivities (Scheme 3). With the exception of the 12-membered macrocycle **5a**, the remaining macrocycles were isolable. As the ring size increases, the reactivities decrease markedly. The largest 18-membered macrocycle does not

Received: October 1, 2015
Published: October 14, 2015

DOI: 10.1021/acs.joc.5b02288
J. Org. Chem. 2015, 80, 11039−11047

Scheme 2. Experimental Data on TADA Reactions

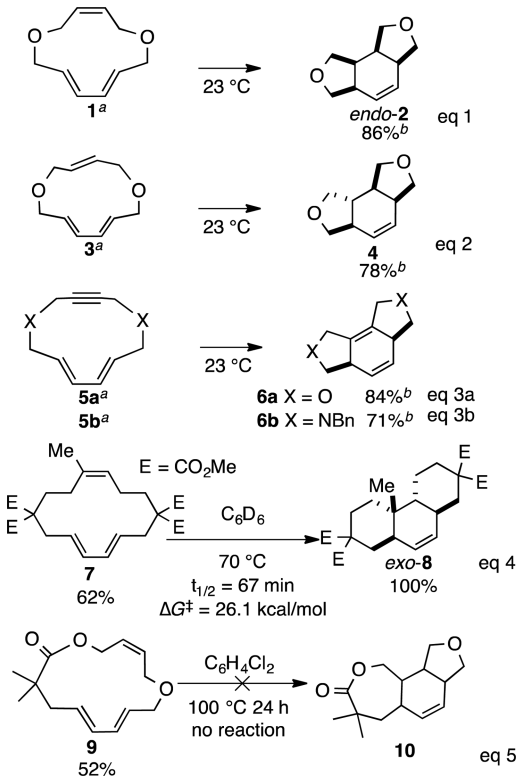

[a]12-membered macrocycles were not isolated. [b]Yields are for two steps from the macrocyclization of the acyclic bisboronates.

Scheme 3. Experimental Data on a Series of TADA Reactions[13]

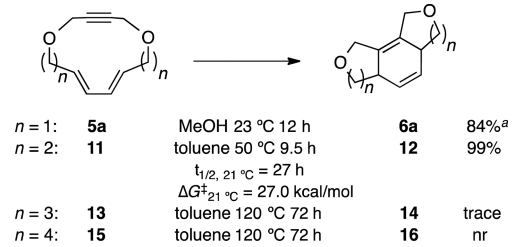

[a]Yield is for two steps from the macrocyclization of the acyclic dienynyl bisboronate.

undergo a TADA reaction. We also observed high reactivities for 12-membered macrocycles containing either alkene (**1** and **3**) or alkyne (**5a,b**) dienophiles.[12,13] The rates of Diels–Alder reactions are usually lower for macrocycles with alkyne dienophiles due to the higher LUMO energies of the dienophiles, but both alkenes and alkynes react readily in these cases.[14]

Kinetic experiments for the 14-membered trienic hydrocarbon macrocycle **7** (Scheme 2) and for the 14-membered dienynic dioxa macrocycle **11** (Scheme 3) were carried out, and the experimental reaction barriers were found to be 26.1 and 27.0 kcal/mol, respectively, on the basis of their half-lives.[12,13]

Although the reactivities of the *cis*/*trans* isomers of C14 trienes have been explored previously, there have been few systematic theoretical studies of TADA reactivities concerning the effects of ring size, and no work has been done on how the types of atoms in the macrocycles modulate reactivities.[15−17] We studied the energetics and transition structures of this series of TADA reactions in order to delineate the origins of the reactivities and stereoselectivities.

METHODS

Optimizations and frequency calculations were computed using the B3LYP density functional theory with the 6-31+G(d,p) basis set implemented in Gaussian 09 Revision D.01.[18] The D2 version of Grimme's dispersion model was used to correct for dispersion energies in the calculations.[19] Single-point energies were calculated at the M06-2X level using the 6-311+G(d,p) basis set. While B3LYP provides accurate optimized geometries, it overestimates reaction barriers for pericyclic reactions.[20] Performing single-point energy calculations with M06-2X on B3LYP optimized structures gives results in better agreement with experimental data without resorting to higher levels of theory.[21] All stationary points were verified as minima or first-order saddle points by a vibrational frequency analysis. All of the free energies are reported in kcal/mol for 1 atm and at 298.15 K.

Conformational searches were carried out with MacroModel from Schrödinger using MMFF with an energy window of 20 kcal/mol.[22] The 10 lowest energy conformers were optimized with B3LYP-D2/6-31+G(d,p) to locate the global minimum for each reaction. Conformations of transition structures are sampled by constrained searches. All graphics on optimized structures were generated with CYLview.[23]

RESULTS AND DISCUSSION

The computed barriers ($\Delta G^{\ddagger}$) for experimental results shown in Scheme 2 for six TADA reactions (eqs 1−5) are given in Table 1. The barriers for 12-membered substrates (eqs 1−3b) are below 20 kcal/mol and thus are expected to be reactive at room temperature. This is consistent with the experimental observation that 12-membered substrates were not isolable under the conditions in which they were generated. Macrocycle **7** (eq 4) undergoes a TADA reaction with a computed barrier of 27.2 kcal/mol in benzene at 343 K and 26.7 kcal/mol in the gas phase at room temperature, which is in good agreement with the experimental barrier of 26.1 kcal/mol. Macrocycle **9** in eq 5 has a high computed barrier of at least 30 kcal/mol and does not undergo a TADA reaction. Overall, our initial computational results are consistent with the experimental observations.

Table 1. Computed Activation Free Energies and Stereoselectivities

	equation					
	1	2	3a	3b	4	5
$\Delta G^{\ddagger}$ [a]	15.7	17.5	12.3	12.2	26.7, 27.2[c]	32.5, 30.0[c]
$\Delta\Delta G^{\ddagger}$ [b]	3.4				−2.0	

[a]Energies are calculated at the M06-2X/6-311+G(d,p)//B3LYP-D2/6-31+G(d,p) level and are reported in kcal/mol in the gas phase. [b]$\Delta\Delta G^{\ddagger} = \Delta G^{\ddagger}_{exo} - \Delta G^{\ddagger}_{endo}$. [c]Energies are calculated with the solvents and temperatures specified in Scheme 2.

There are two diastereomeric transition states for the TADA reaction of macrocycle **1**, and the energy difference between the *endo* and the *exo* pathways is 3.4 kcal/mol in favor of the *endo* transition state. This is consistent with the stereoselectivity observed experimentally. The forming five-membered rings in all of the transition structures adopt envelope conformations exclusively (Figure 1). The stereochemistry is explained by the lower energy of the *cis*-ring junctions in the *endo* transition state. This preference is more pronounced in the product, and

DOI: 10.1021/acs.joc.5b02288
J. Org. Chem. 2015, 80, 11039−11047

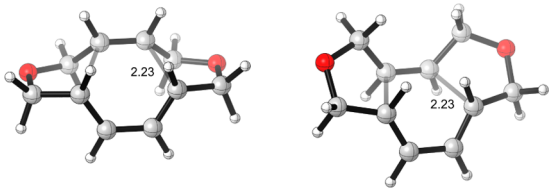

1-*endo*-TS
$\Delta G^{\ddagger} = 15.7$
$\Delta G^{\circ} = -42.0$

1-*exo*-TS
$\Delta G^{\ddagger} = 19.1$
$\Delta G^{\circ} = -29.2$

Figure 1. *Endo* and *exo* transition structures of the TADA reaction of **1** to **2**.

the *cis*-fused [5,6,5]-tricycle is 12.8 kcal/mol lower in energy than the *trans*-fused tricycle.

The stereoselectivities of TADA reactions of 14-membered macrocycles have been studied theoretically and experimentally by Deslongchamps and co-workers.[17] For the TADA reaction of the 14-membered macrocycle **7**, the 6-membered rings formed by the tethers preferentially adopt chair conformations (Figure 2). Transition structures with more than one boat

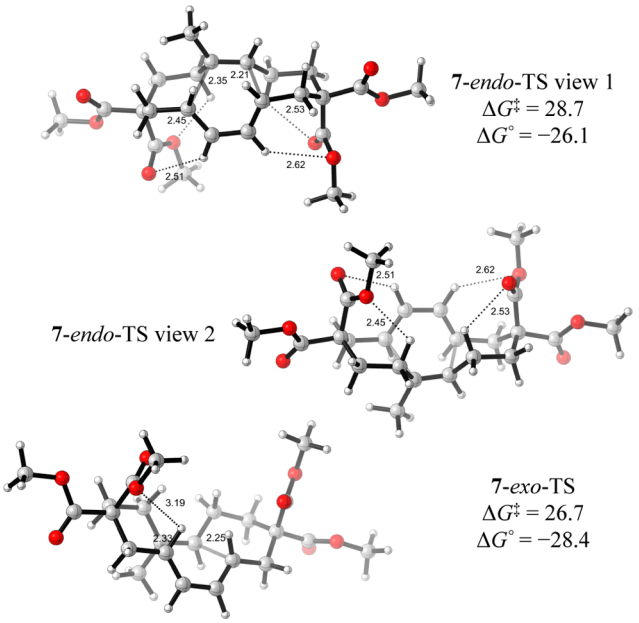

Figure 2. *endo* and *exo* transition structures of the TADA reaction of **7** to **8**.

conformation (for details, see the Supporting Information) are at least 3.1 kcal/mol less stable than the chair–boat–chair conformers. The computed energy difference between *endo* and *exo* transition states is 2.0 kcal/mol in favor of the *exo* pathway. Although both transition states adopt chair–boat–chair conformations, there are steric clashes between the carbonyl oxygen atoms of the axial methyl esters and the diene hydrogens in the *endo* transition state, as revealed by view 2 in Figure 2. These steric clashes are not found in the *exo* transition state.

To further understand the differences in reactivities among the transannular Diels–Alder reactions, we compared these results to those for simple models. We first studied a series of four bimolecular and six intramolecular Diels–Alder reactions (Tables 2 and 3). These substrates were chosen because they share the same diene and dienophile moieties with the transannular substrates. The two common motifs, namely the

Table 2. Computed Activation Parameters for Bimolecular Diels–Alder Reactions Modeled in This Work

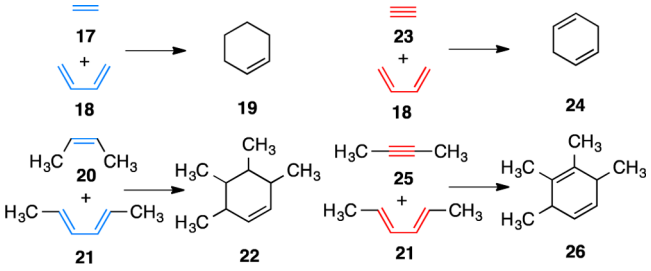

	$\Delta E^{\ddagger a}$	$\Delta H^{\ddagger a}$	$-T\Delta S^{\ddagger a}$	$\Delta G^{\ddagger a}$
17/**18**-TS	19.7	20.9	13.5	34.4
20/**21**-*endo*-TS	21.2	22.4	15.9	38.3
20/**21**-*exo*-TS	24.3	25.4	15.2	40.6
23/**18**-TS	21.3	21.8	11.5	33.3
25/**21**-TS	28.5	29.3	15.1	44.4

[a]Energies are calculated at the M06-2X/6-311+G(d,p)//B3LYP-D2/6-31+G(d,p) level and are reported in kcal/mol in the gas phase.

Table 3. Computed Activation Parameters for Model Intramolecular Diels–Alder Reactions

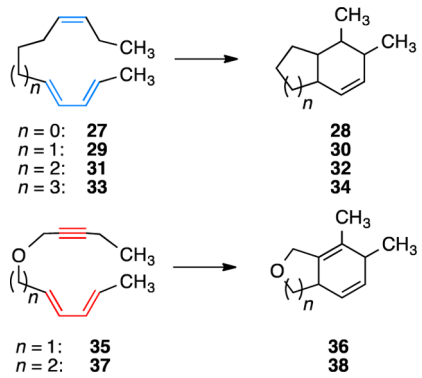

n		$\Delta E^{\ddagger a}$	$\Delta H^{\ddagger a}$	$-T\Delta S^{\ddagger a}$	$\Delta G^{\ddagger a}$
0	**27**-*endo*-TS	38.8	37.7	3.3	41.0
	27-*exo*-TS	40.9	40.0	3.4	43.4
1	**29**-*endo*-TS	26.0	25.4	3.4	28.8
	29-*exo*-TS	28.7	28.1	3.2	31.3
2	**31**-*endo*-TS	23.8	23.4	4.7	28.1
	31-*exo*-TS	25.4	24.8	4.1	28.9
3	**33**-*endo*-TS	30.2	29.9	3.7	33.6
	33-*exo*-TS	33.4	33.1	3.6	36.7
1	**35**-TS	25.8	24.9	3.3	28.3
2	**37**-TS	29.3	28.6	4.1	32.7

[a]Energies are calculated at the M06-2X/6-311+G(d,p)//B3LYP-D2/6-31+G(d,p) level and are reported in kcal/mol in the gas phase.

triene and the dienyne, are color coded in blue and red, respectively.

Table 2 shows four bimolecular reactions varying in the dienophile (alkenyl versus alkynyl) and in the extent of substitution of the reactive component (hydrogen versus methyl group). Their energetics are also given Table 2. The common theme in bimolecular Diels–Alder reactions is their large $-T\Delta S^{\ddagger}$ terms (12–16 kcal/mol). For the unsubstituted substrates **17**/**18** and **23**/**18**, which only differ in the dienophile, the activation barriers of 34.4 and 33.3 kcal/mol, respectively, are similar. When a methyl group is added to each end of the reactive compoment, the barriers are substantially

DOI: 10.1021/acs.joc.5b02288
J. Org. Chem. 2015, 80, 11039–11047

higher (40.6 and 44.4 kcal/mol) due to steric hindrance in the transition states. The reaction with the alkynyl dienophile is enthalpically less favorable, which is well-known experimentally.[14,21] For the reaction with **20**/**21**, the *endo* transition state is 2.3 kcal/mol more stable than the *exo* state.

The six intramolecular reactions and their energetics are shown in Table 3. Both the hydrocarbon and the oxadienynic series are shown. The substrates within each series vary in the length of the tether. In general, their entropy terms are approximately 10 kcal/mol lower than those of the bimolecular reactions. The great decrease in the entropy term from 12−16 kcal/mol to 3−5 kcal/mol is consistent with the reduced translational and rotational entropy cost of unimolecular processes relative to bimolecular reactions. The intramolecular reactions have activation enthalpies that are higher than those of the bimolecular reactions depending on the tether length. The increase in reactivities of intramolecular Diels−Alder reactions is entropy-controlled.

We have modeled 13 TADA reactions to systematically investigate the factors controlling their reactivities (Scheme 4). They are designed to model the effects of tether length, alkenyl versus alkynyl dienophile, and the types of atoms in the tethers.

Scheme 4. TADA Reactions Studied Computationally

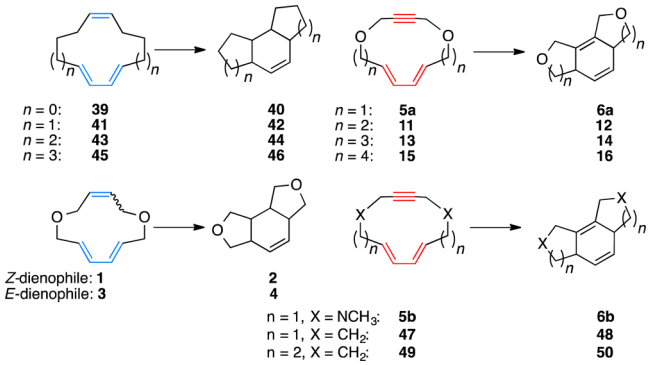

To quantify how tether length, types of atoms, and types of dienophile affect activation enthalpies in TADA reactions, we used a modified variant of the distortion-interaction model to analyze these transannular cycloadditions. The distortion-interaction model was developed to study bimolecular reactions but has been applied to intramolecular cycloadditions.[24−26] The activation energy, $\Delta E^{\ddagger}$, is dissected into two parts, namely the distortion energy $\Delta E^{\ddagger}_{d}$ and the interaction energy $\Delta E^{\ddagger}_{i}$: $\Delta E^{\ddagger} = \Delta E^{\ddagger}_{d} + \Delta E^{\ddagger}_{i}$. $\Delta E^{\ddagger}_{d}$ is defined as the total energy required to distort the geometry of each isolated reactant into the geometry of the transition state without allowing interaction between reactants. $\Delta E^{\ddagger}_{i}$ is the interaction energy between the reacting components in the transition state, which is determined by subtracting the distortion energy from the activation energy.

We modified the model to treat unimolecular systems such as TADA reactions as employed previously to study other intramolecular cycloadditions.[26] The substrate contains two portions: the reactive components and the tether(s) that link them together. We removed the tethers and capped the carbon with a hydrogen atom at 1.07 Å (Scheme 5). The result of this procedure yields diene and dienophile fragments that are separate from each other but still possess the geometries they adopt in the original transannular reactions. $\Delta E^{\ddagger}_{app}$, or the apparent activation energy, refers to the energy difference between the interacting transition state structures and the

Scheme 5. Modified Distortion-Interaction Model That Allows Analysis of Unimolecular Reactions

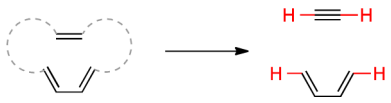

reactant structures. The differences between $\Delta E^{\ddagger}$ and $\Delta E^{\ddagger}_{app}$ are the approximate distortion energies of the tethers, $\Delta E^{\ddagger}_{tether}$.

Table 4 summarizes the results of the distortion-interaction analysis for the methylated model bimolecular reaction and for

Table 4. Distortion-Interaction Analysis on Bimolecular and Intramolecular Diels−Alder Reactions[a]

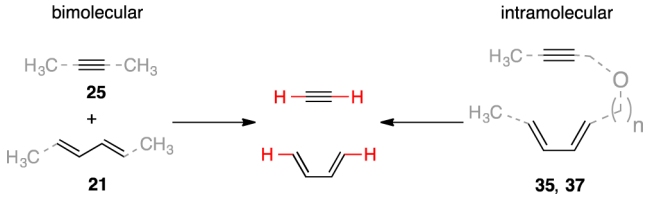

	reaction			
	BMDA-**18**/**23**	BMDA-**21**/**25**	IMDA-**35** (n = 1)	IMDA-**37** (n = 2)
$\Delta E^{\ddagger}$		28.5	25.8	29.3
$\Delta E^{\ddagger}_{d,diene}$	17.6	16.7	19.0	15.8
$\Delta E^{\ddagger}_{d,dienophile}$	11.6	18.6	15.2	21.5
$\Delta E^{\ddagger}_{d,total}$	29.1	35.3	34.2	37.3
$\Delta E^{\ddagger}_{tether}$		5.3	2.3	5.6
$\Delta E^{\ddagger}_{i}$	−7.8	−12.0	−10.6	−13.6

[a]Values are given in kcal/mol.

the intramolecular reactions. In general, more energy is required to distort the diene and dienophile from the reactant geometry to the transition state geometry for methylated systems than for nonmethylated systems due to steric effects. In comparison to the prototypical bimolecular model, the methyl-substituted reaction has a total distortion energy that is 6 kcal/mol higher. The difference of 5.3 kcal/mol between $\Delta E^{\ddagger}$ and $\Delta E^{\ddagger}_{app}$ suggests there is strain carried by the methyl groups, which come close in the transition structure. For the intramolecular reactions, the total distortion energies of the diene and the dienophile are higher than those of the parent bimolecular reactions. In addition, the tethers are also strained in the transition states ($\Delta E^{\ddagger} - \Delta E^{\ddagger}_{app} > 0$). Given that, substrate **35**, with less tether strain, is more reactive.

(1). Tether Length. Scheme 4 shows 13 model TADA reactions that were investigated in this work. We first analyze two series that demonstrate how ring size influences TADA reactivity. The energetics are summarized in Tables 5 and 6. For reactions with diastereomeric (*endo* versus *exo*) pathways, the lowest values are shown. The series of hydrocarbon macrocycles in Table 5 ranges from 10- to 16-membered rings, and the dioxa macrocyclic series in Table 6 ranges from 12- to 18-membered rings. For the series of dioxa macrocycles, we compare our computational predictions with Merlic's experimental results. The computed barrier of 28.0 kcal/mol for the reaction with **11** is in good agreement with the experimentally measured barrier of 27.0 kcal/mol.

In both series, the 12-membered macrocyclic substrates have the lowest activation barriers. The 12-membered hydrocarbon **41** has an activation free energy of 20.4 kcal/mol, while the

DOI: 10.1021/acs.joc.5b02288
J. Org. Chem. 2015, 80, 11039−11047

Table 5. Activation Parameters of a Series of Model Reactions with Trienic Macrocycles To Demonstrate the Effects of Tether Length on TADA Reaction Rates

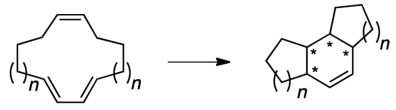

n = 0:	**39**	**40**
n = 1:	**41**	**42**
n = 2:	**43**	**44**
n = 3:	**45**	**46**

	$\Delta H^{\ddagger}$ [a]	$-T\Delta S^{\ddagger}$ [a]	$\Delta G^{\ddagger}$ [a]
39-*endo*-TS (10)[b]	26.9	1.3	28.2
41-*endo*-TS (12)[b]	19.6	1.6	21.2
43-*exo*-TS (14)[b]	21.1	2.5	23.6
45-*endo*-TS (16)[b]	30.6	3.1	33.7

[a]Energies are calculated at the M06-2X/6-311+G(d,p)//B3LYP-D2/6-31+G(d,p) level and are reported in kcal/mol. [b]The size of the macrocycle is given in parentheses.

Table 6. Activation Parameters of a Series of Model Reactions with Dioxa Macrocycles To Demonstrate the Effects of Tether Length on TADA Reaction Rates

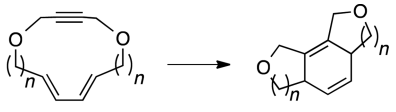

n = 1:	**5a**	**6a**
n = 2:	**11**	**12**
n = 3:	**13**	**14**
n = 4:	**15**	**16**

	$\Delta H^{\ddagger}$[a]	$-T\Delta S^{\ddagger}$[a]	$\Delta G^{\ddagger}$[a]	T (°C), yield (%)[b]
5a-TS (12)[c]	10.8	1.8	12.6	room temp, 84[d]
11-TS (14)[c]	25.9	2.1	28.0	50, 99
13-TS (16)[c]	36.1	1.8	37.9	120, trace
15-TS (18)[c]	38.9	2.7	41.6	120, nr

[a]Energies are calculated at the M06-2X/6-311+G(d,p)//B3LYP-D2/6-31+G(d,p) level and are reported in kcal/mol. [b]Experimental yields and reaction temperatures. [c]The size of the macrocycle is given in parentheses. [d]Yield is for two steps from the macrocyclization of the acyclic dienyne.

dioxa analogue **5a** has a barrier of only 12.6 kcal/mol. Both substrates form [5,6,5]-fused tricyclic products. Note that while the activation entropies range from 1 to 3 kcal/mol for all reactions, the activation enthalpies for the 12-membered substrates are considerably lower than those of most larger substrates, which is thus responsible for the rate enhancement.

The 10-membered and 14-membered substrates are also reactive at ambient or slightly elevated temperatures, with a barrier range of 23−28 kcal/mol. Macrocycles of 16 atoms or more do not undergo the TADA reaction readily. The computed barriers for the dioxa macrocycles **5a**, **11**, **13**, and **15** correspond well with the experimental yields and reaction conditions. Figure 3 shows the computed lowest energy transition structures for both model series.

The distortion-interaction analysis for bimolecular and intramolecular Diels−Alder reactions was given in Table 4. We now present similar results for the TADA reactions. Table 7 compares trienic macrocycles **39**, **41**, **43**, and **45** to the prototypical bimolecular reaction between 2-butene (**20**) and 2,4-hexadiene (**21**). For all cases, there are two factors governing the reactivities of TADA reactions: the total distortion energy of the reactive components and the tether strain change from the reactant to the transition state geometry

Table 7. Distortion-Interaction Analysis on TADA Reactions 39−45[a]

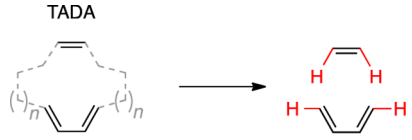

39, **41**, **43**, **45**

	reaction				
	BMDA-**20**/**21**	**39**-*endo* (n = 0)	**41**-*endo* (n = 1)	**43**-*exo* (n = 2)	**45**-*endo* (n = 3)
$\Delta E^{\ddagger}_{d,diene}$	20.7	15.1	13.4	16.8	21.6
$\Delta E^{\ddagger}_{d,dienophile}$	11.4	8.0	7.7	10.1	16.8
$\Delta E^{\ddagger}_{d,total}$	32.1	23.1	21.0	26.9	38.3
$\Delta E^{\ddagger}_{i}$	−12.5	−6.6	−7.9	−9.3	−15.4
$\Delta E^{\ddagger}_{app}$	19.6	16.5	13.1	17.6	22.9
$\Delta E^{\ddagger}$	21.2	28.3	20.2	22.3	30.5
$\Delta E^{\ddagger}_{d,tether}$	1.6	11.8	7.1	4.7	7.6

[a]Values are given in kcal/mol.

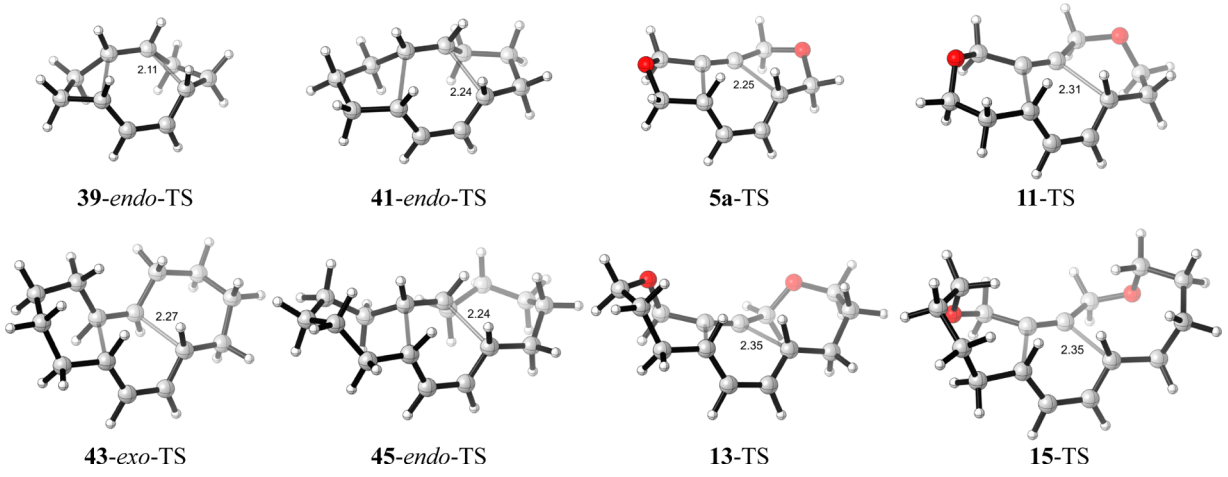

39-*endo*-TS **41**-*endo*-TS **5a**-TS **11**-TS

43-*exo*-TS **45**-*endo*-TS **13**-TS **15**-TS

Figure 3. Transition structures of TADA reactions.

DOI: 10.1021/acs.joc.5b02288
J. Org. Chem. 2015, 80, 11039−11047

(both indicated in green). All TADA reactions here have increased tether strain in the transition states, which shows that the tethers contribute negatively to reactivities ($\Delta E^{\ddagger} - \Delta E^{\ddagger}_{app} = \Delta E^{\ddagger}_{d,tether} > 0$). The reaction of **39** has the highest tether strain, because two four-membered rings are formed in the product. The reaction of **43** has the least tether strain, as two cyclohexane rings are formed in the most stable chair conformation. Despite this, the reaction of **43** is not the most facile. The TADA reaction of **41** is the most facile in the series because it has the lowest total distortion energy and a reasonable tether strain of 7.1 kcal/mol.

To illustrate this point, we compare the reactions of **39** and **43**. The total distortion in the reaction of the former is slightly smaller, but its tether strain is significantly larger. When both factors are weighed, the reaction of **43** is faster. Substrate **45** does not undergo aTADA reaction due to the high diene–dienophile distortion energy and high tether strain.

The unsymmetrical 13-membered macrocycle should show reactivity between those of the 12-membered and 14-membered macrocycles. Indeed, the trienic 13-membered macrocycle is predicted to undergo a TADA reaction via the *endo* pathway with a barrier of 21.9 kcal/mol (for details, see the Supporting Information).

Table 8 shows the distortion-interaction analysis for the TADA reactions of dioxa macrocycles **5a**, **11**, **13**, and **15**. For the reaction of **5a**, which forms a [5,6,5]-fused tricyclic product, the energy required to distort the reactive components to the transition state geometry is 23.1 kcal/mol, which is 12.2 kcal/mol lower than that of the bimolecular reaction. The three-atom tethers bring the diene and the dienophile into close proximity to allow for a more facile Diels–Alder reaction. In addition, the tether strain going from the reactant to the transition state geometry is reduced ($\Delta E^{\ddagger}_{d,tether} = -4.1$). As a result, this reaction has a very low barrier ($\Delta G^{\ddagger}$ = 12.6 kcal/mol). For the reactions of **11**, **13**, and **15**, as the tether length increases, the total distortion energy increases to be greater than that of the bimolecular reaction, although that is partially compensated by the interaction energy. In fact, the presence of longer tethers is enthalpically worse than the case of no tether at all. Moreover, the $\Delta E^{\ddagger}_{d,tether}$ term suggests that the longer tethers are building up strain in the transition states ($\Delta E^{\ddagger}_{d,tether}$ > 0 kcal/mol).

Table 8. Distortion-Interaction Analysis on TADA Reactions 5a and 11–15[a]

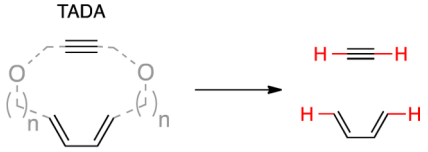

5a, **11**, **13**, **15**

	reaction				
	BMDA-**21**/**25**	**5a** (n = 1)	**11** (n = 2)	**13** (n = 3)	**15** (n = 4)
$\Delta E^{\ddagger}_{d,diene}$	16.7	13.7	12.6	13.6	15.9
$\Delta E^{\ddagger}_{d,dienophile}$	18.6	9.4	22.2	17.2	26.9
$\Delta E^{\ddagger}_{d,total}$	35.3	23.1	34.8	30.7	42.8
$\Delta E^{\ddagger}_{i}$	−12.0	−7.3	−12.7	−7.9	−12.7
$\Delta E^{\ddagger}_{app}$	23.2	15.9	21.1	22.8	30.0
$\Delta E^{\ddagger}$	28.5	11.8	26.4	37.7	40.0
$\Delta E^{\ddagger}_{d,tether}$	5.3	−4.1	4.3	14.9	10.0

[a]Values are given in kcal/mol.

A TADA reaction is most facile when the diene and the dienophile need to distort minimally due to the presence of the two tethers and when the two tethers are least strained going from the reactant to the transition state geometries. Only the TADA reaction of **5a** meets both criteria and is hence most reactive. TADA reactions that satisfy only one criterion such as those of **41** and **43** are less reactive, and those with high distortion energies for both the reactive components and the tethers are enthalpically disfavored. TADA substrates with longer tethers exhibit distortion energies similar to or greater than those of the intermolecular reactions, along with strain built up in the tethers in the transition states. However, these reactions are still faster than intermolecular reactions due to the elimination of translational and conformational entropy.

(2). Types of Atoms within the Macrocycle. Merlic and co-workers synthesized macrocyclic diethers and diamines that also underwent facile TADA reactions. The heteroatoms can effectively shrink the size of the macrocycles due to shorter C–X bonds. Calculations show that the 12-membered hydrocarbon macrocyclic triene **41** and the oxygen-containing triene **1** have activation free energies of 21.2 and 15.7 kcal/mol, respectively. The dienyne **47**, the oxygen-containing **5a**, and the nitrogen-containing **5b** have activation free energies of 14.2, 12.6, and 12.2 kcal/mol, respectively. We calculate that for 12-membered macrocycles, replacing carbon atoms with heteroatoms such as oxygen and nitrogen increases the reaction rate by 10–1000-fold (Table 9).

Table 9. Activation Parameters of Two Series of Modeled Reactions To Demonstrate the Effect of Heteroatoms in 12-Membered Macrocycles on TADA Reactivity

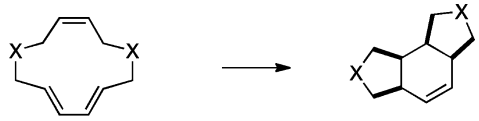

41 X = CH_2
1 X = O

	$\Delta H^{\ddagger a}$	$-T\Delta S^{\ddagger a}$	$\Delta G^{\ddagger a}$
41-*endo*-TS	19.6	1.6	21.2
1-*endo*-TS	14.4	1.3	15.7

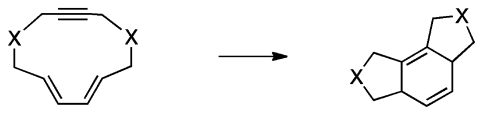

47 X = CH_2
5a X = O
5b X = NMe

	$\Delta H^{\ddagger a}$	$-T\Delta S^{\ddagger a}$	$\Delta G^{\ddagger a}$
47-TS	12.6	1.6	14.2
5a-TS	10.8	1.8	12.6
5b-TS	10.6	1.6	12.2

[a]Reported energies are M06-2X/6-311+G(d,p)//B3LYP-D2/6-31+G-(d,p) energies in kcal/mol in the gas phase.

DOI: 10.1021/acs.joc.5b02288
J. Org. Chem. 2015, 80, 11039–11047

Table 10 shows the distortion-interaction analysis for the two series of TADA reactions. As X changes from a carbon atom to a heteroatom, the decrease in the total distortion of the diene and the dienophile is accompanied by a decrease of favorable interaction between the two reactive parts with comparable magnitudes (2−3 kcal/mol). However, the distortion of the tether is greatly reduced (2−5.6 kcal/mol) when the heteroatom is part of the ring. The incorporation of heteroatoms enhances TADA reaction rates by reducing the distortion of the tethers built up in the transition states.

Table 10. Distortion-Interaction Analysis Explaining the High Reactivities with Heteroatoms in 12-Membered Macrocycles[a]

	$\Delta E^{\ddagger}$	$\Delta E^{\ddagger}_{d,total}$	$\Delta E^{\ddagger}_{i}$	$\Delta E^{\ddagger}_{d,tether}$
41-*endo*-TS	20.2	21.0	−7.9	7.1
1-*endo*-TS	15.1	19.3	−5.7	1.5
47-TS	14.0	26.0	−10.2	−1.8
5a-TS	11.8	23.1	−7.3	−4.1
5b-TS	12.1	23.5	−7.6	−3.8

[a]Values are given in kcal/mol.

(3). Alkene versus Alkyne Dienophile. As previously shown, Diels−Alder reactions with alkyne dienophiles are enthalpically less favorable.[21] Table 11 compares the activation parameters for the TADA reactions of the alkene and the alkyne 14-membered macrocycles. The barrier for the alkyne-containing macrocycle is much higher than that for the alkene-containing macrocycle, as expected (31.8 versus 22.6 kcal/mol). The distortion-interaction analysis shows that the distortions for both the reactive components and the tethers are higher in the alkyne macrocycle (Table 12).

Table 11. Activation Parameters of Alkene vs Alkyne 14-Membered Macrocycles

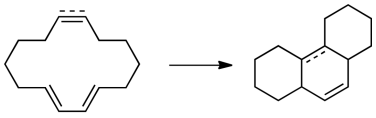

43 alkene
49 alkyne

	$\Delta H^{\ddagger a}$	$-T\Delta S^{\ddagger a}$	$\Delta G^{\ddagger a}$
(*Z*)-**43**-*exo*-TS	20.4	2.2	22.6
49-TS	30.1	1.7	31.8

[a]Reported energies are M06-2X/6-311+G(d,p)//B3LYP-D2/6-31+G(d,p) energies in kcal/mol in the gas phase.

For 12-membered macrocycles, macrocycles with a *trans*-alkene dienophile are roughly 100-fold less reactive than those with a *cis*-alkene, in accord with literature examples (Table 13).[16,27] However, substrates possessing alkyne dienophiles are 10^2−10^5-fold more reactive than those involving *cis*-alkene dienophiles. Table 14 shows that although distortions of the reactive parts of macrocycles **47** and **5a** are higher, which is expected for alkyne dienophiles, the distortions of the tethers are significantly lower by 5−9 kcal/mol in comparison to their *cis*-alkene dienophile counterparts (**41** and **1**). This is because the 12-membered cyclodienyne has more strain release than 12-membered cyclotriene in the cycloaddition transition state.

Table 12. Distortion-Interaction Analysis for Two TADA Reactions of 14-Membered Macrocycles[a]

	$\Delta E^{\ddagger}$	$\Delta E^{\ddagger}_{d,total}$	$\Delta E^{\ddagger}_{i}$	$\Delta E^{\ddagger}_{d,tether}$
(*Z*)-**43**-*exo*-TS	22.3	26.9	−9.3	4.7
49-TS	31.0	34.8	−12.7	8.9

[a]Values are given in kcal/mol.

Table 13. Activation Parameters of Two Series of Modeled Reactions To Demonstrate the Effect of Dienophile Types in 12-Membered Macrocycles on TADA Reactivity

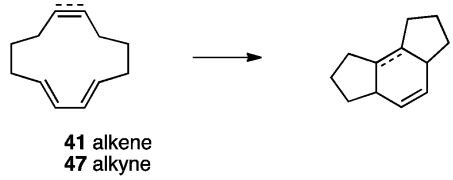

41 alkene
47 alkyne

	$\Delta H^{\ddagger a}$	$-T\Delta S^{\ddagger a}$	$\Delta G^{\ddagger a}$
41-*endo*-TS	19.6	1.6	21.2
47-TS	12.6	1.6	14.2

1 *cis*-alkene
3 *trans*-alkene
5a alkyne

	$\Delta H^{\ddagger a}$	$-T\Delta S^{\ddagger a}$	$\Delta G^{\ddagger a}$
1-*endo*-TS	14.4	1.3	15.7
3-TS	15.7	1.8	17.5
5a-TS	10.8	1.8	12.6

[a]Reported energies are M06-2X/6-311+G(d,p)//B3LYP-D2/6-31+G(d,p) energies in kcal/mol in the gas phase.

Table 14. Distortion-Interaction Analysis Explaining the High Reactivities for Alkyne-Containing 12-Membered Macrocycles[a]

	$\Delta E^{\ddagger}$	$\Delta E^{\ddagger}_{d,total}$	$\Delta E^{\ddagger}_{i}$	$\Delta E^{\ddagger}_{d,tether}$
41-*endo*-TS	20.2	21.0	−7.9	7.1
47-TS	14.0	26.0	−10.2	−1.8
1-*endo*-TS	15.1	19.3	−5.7	1.5
3-TS	16.3	24.0	−8.0	0.3
5a-TS	11.8	23.1	−7.3	−4.1

[a]Values are given in kcal/mol.

The rate enhancement with alkyne dienophiles and/or heteroatoms in 12-membered macrocycles summarized in Figure 4 is an exception rather than a general trend. For larger macrocycles, the rate enhancements were not observed. The effect of alkyne dienophiles in larger rings resembles that for the bimolecular and intramolecular Diels−Alder reactions, decreasing reactivity.

DOI: 10.1021/acs.joc.5b02288
J. Org. Chem. 2015, 80, 11039−11047

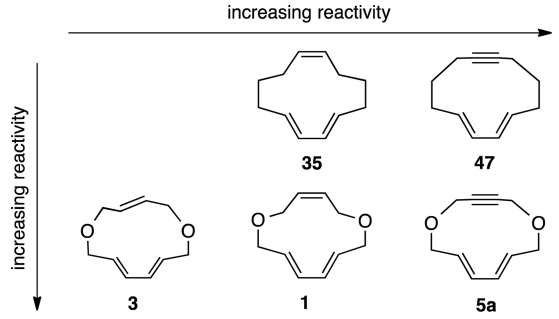

Figure 4. TADA reactivity trends for 12-membered macrocycles.

CONCLUSIONS

The reactivities of macrocyclic trienes and dienynes in TADA reactions have been systematically investigated. The most reactive TADA substrates benefit from two factors: lowering of the distortion energies of the diene and dienophile in comparison to bimolecular and intramolecular reactions due to the linking tethers and strain release of the tethers in the transition structures. Among the macrocycles we studied, 12-membered rings undergo the most facile TADA reactions due to favorable enthalpy. Within 12-membered rings, the presence of heteroatoms in the tethers and alkynyl dienophiles increases the reactivities by up to 5 orders of magnitude relative to the all hydrocarbon trienic macrocycles.

ASSOCIATED CONTENT

Supporting Information

The Supporting Information is available free of charge on the ACS Publications website at DOI: 10.1021/acs.joc.5b02288.

Complete sets of TSs for the TADA reactions carried out experimentally (**TS-1**, **3**, **5**, **7**, **9**) and for the model bimolecular (**TS-17/18**, **TS-20/21**, **TS-23/18**, and **TS-25/21**), intramolecular (**TS-27**, **29**, **31**, **33**, **35**, **37**), and transannular (**TS-39**, **41**, **43**, **45**, **47**, **49**, **51**) Diels–Alder reactions, conformers of 7-*exo*-**TS**, and Cartesian coordiates and thermodynamic parameters (in hartree) of all stationary points (PDF)

AUTHOR INFORMATION

Corresponding Authors

*E-mail for C.A.M.: merlic@chem.ucla.edu.
*E-mail for K.N.H.: houk@chem.ucla.edu.

Notes

The authors declare no competing financial interest.

ACKNOWLEDGMENTS

We are grateful to the National Science Foundation for financial support of this research (CHE-1059084 and CHE-1361104). Calculations were performed on the Hoffman2 cluster at UCLA and the Extreme Science and Engineering Discovery Environment (XSEDE), which is supported by the National Science Foundation (OCI-1053575). Experiments carried out in the Merlic group are supported by the American Chemical Society Petroleum Research Fund (48564-AC1).

REFERENCES

(1) Diels, O.; Alder, K. *Justus Liebigs Ann. Chem.* **1928**, *460*, 98.
(2) DeWitt, E. J.; Lester, C. T.; Ropp, G. A. *J. Am. Chem. Soc.* **1956**, *78*, 2101.
(3) Alder, K.; Jacobs, G. *Chem. Ber.* **1953**, *86*, 1528.
(4) Sauer, J.; Wiest, H. *Angew. Chem., Int. Ed. Engl.* **1962**, *1*, 269.
(5) For reviews on intramolecular Diels–Alder reactions, see: (a) Fallis, A. G. *Can. J. Chem.* **1984**, *62*, 183. (b) Craig, D. *Chem. Soc. Rev.* **1987**, *16*, 187. (c) Oppolzer, W. Intermolecular Diels-Alder Reactions. In *Comprehensive Organic Synthesis - Selectivity, Strategy and Efficiency in Modern Organic Chemistry*; Trost, B. M., Fleming, I., Eds.; Pergamon: New York, 1991; Vol. *5*, pp 315–400. (d) Roush, W. R. Intramolecular Diels-Alder Reactions. In *Comprehensive Organic Synthesis - Selectivity, Strategy and Efficiency in Modern Organic Chemistry*; Trost, B. M., Fleming, I., Eds.; Pergamon: New York, 1991; Vol. *5*, pp 531–551. (e) Ciganek, E. In *Organic Reactions*; Wiley: Hoboken, NJ, 2004.
(6) Diedrich, M. K.; Klärner, F.-G.; Beno, B. R.; Houk, K. N.; Senderowitz, H.; Still, W. C. *J. Am. Chem. Soc.* **1997**, *119*, 10255.
(7) For reviews, see: (a) Marsault, E.; Toró, A.; Nowak, P.; Deslongchamps, P. *Tetrahedron* **2001**, *57*, 4243. (b) Nicolaou, K. C.; Snyder, S. A.; Montagnon, T.; Vassilikogiannakis, G. *Angew. Chem., Int. Ed.* **2002**, *41*, 1668. (c) Juhl, M.; Tanner, D. *Chem. Soc. Rev.* **2009**, *38*, 2983. (d) Reyes, E.; Uria, U.; Carrillo, L.; Vicario, J. L. *Tetrahedron* **2014**, *70*, 9461.
(8) For application examples, see: (a) Xu, Y.-C.; Cantin, M.; Deslongchamps, P. *Can. J. Chem.* **1990**, *68*, 2137. (b) Takao, K.-I.; Munakata, R.; Tadano, K.-I. *Chem. Rev.* **2005**, *105*, 4779. (c) Tortosa, M.; Yakelis, N. A.; Roush, W. R. *J. Am. Chem. Soc.* **2008**, *130*, 2722. (d) Li, Y.; Pattenden, G. *Tetrahedron Lett.* **2011**, *52*, 2088.
(9) Lamothe, S.; Ndibwami, A.; Deslongchamps, P. *Tetrahedron Lett.* **1988**, *29*, 1639.
(10) Ndibwami, A.; Lamothe, S.; Soucy, P.; Goldstein, S.; Deslongchamps, P. *Can. J. Chem.* **1993**, *71*, 714.
(11) Deslongchamps, P.; Pitteloud, R. *Aldrichimica Acta* **1991**, *24*, 43.
(12) Iafe, R. G.; Kuo, J. L.; Hochstatter, D. G.; Saga, T.; Turner, J. W.; Merlic, C. A. *Org. Lett.* **2013**, *15*, 582.
(13) Karabiyikoglu, S.; Merlic, C. A. *Org. Lett.* **2015**, *17*, 4086.
(14) (a) Sauer, J. *Angew. Chem., Int. Ed. Engl.* **1966**, *5*, 211. (b) Liao, W.; Yu, Z.-X. *J. Org. Chem.* **2014**, *79*, 11949. (c) Tang, S.-Y.; Shi, J.; Guo, Q.-X. *Org. Biomol. Chem.* **2012**, *10*, 2673.
(15) Prathyusha, V.; Ramakrishna, S.; Priyakumar, U. D. *J. Org. Chem.* **2012**, *77*, 5371.
(16) Wolfe, S.; Buckley, A. V.; Weinberg, N. *Can. J. Chem.* **2001**, *79*, 1284.
(17) Fortin, S.; Barriault, L.; Dory, Y. L.; Deslongchamps, P. *J. Am. Chem. Soc.* **2001**, *123*, 8210.
(18) Frisch, M. J.; Trucks, G. W.; Schlegel, H. B.; Scuseria, G. E.; Robb, M. A.; Cheeseman, J. R.; Scalmani, G.; Barone, V.; Mennucci, B.; Petersson, G. A.; Nakatsuji, H.; Caricato, M.; Li, X.; Hratchian, H. P.; Izmaylov, A. F.; Bloino, J.; Zheng, G.; Sonnenberg, J. L.; Hada, M.; Ehara, M.; Toyota, K.; Fukuda, R.; Hasegawa, J.; Ishida, M.; Nakajima, T.; Honda, Y.; Kitao, O.; Nakai, H.; Vreven, T.; Montgomery, J. A., Jr.; Peralta, J. E.; Ogliaro, F.; Bearpark, M.; Heyd, J. J.; Brothers, E.; Kudin, K. N.; Staroverov, V. N.; Keith, T.; Kobayashi, R.; Normand, J.; Raghavachari, K.; Rendell, A.; Burant, J. C.; Iyengar, S. S.; Tomasi, J.; Cossi, M.; Rega, N.; Millam, J. M.; Klene, M.; Knox, J. E.; Cross, J. B.; Bakken, V.; Adamo, C.; Jaramillo, J.; Gomperts, R.; Stratmann, R. E.; Yazyev, O.; Austin, A. J.; Cammi, R.; Pomelli, C.; Ochterski, J. W.; Martin, R. L.; Morokuma, K.; Zakrzewski, V. G.; Voth, G. A.; Salvador, P.; Dannenberg, J. J.; Dapprich, S.; Daniels, A. D.; Farkas, O.; Foresman, J. B.; Ortiz, J. V.; Cioslowski, J.; Fox, D. J. *Gaussian 09, revision D.01*; Gaussian Inc., Wallingford, CT, 2013.
(19) Grimme, S. *J. Comput. Chem.* **2006**, *27*, 1787.
(20) Goumans, T. P. M.; Ehlers, A. W.; Lammertsma, K.; Würthwein, E.–U.; Grimme, S. *Chem. - Eur. J.* **2004**, *10*, 6468.
(21) Pieniazek, S.; Clemente, F.; Houk, K. N. *Angew. Chem., Int. Ed.* **2008**, *47*, 7746.
(22) Watts, K. S.; Dalal, P.; Tebben, A. J.; Cheney, D. L.; Shelley, J. C. *J. Chem. Inf. Model.* **2014**, *54*, 2680.
(23) Legault, C. Y. *CYLview, 1.0 b*; Université de Sherbrooke (http://www.cylview.org), 2009.

DOI: 10.1021/acs.joc.5b02288
J. Org. Chem. 2015, 80, 11039–11047

(24) (a) Ess, D. H.; Houk, K. N. *J. Am. Chem. Soc.* **2007**, *129*, 10646. (b) Ess, D. H.; Houk, K. N. *J. Am. Chem. Soc.* **2008**, *130*, 10187. (c) Hayden, A. E.; Houk, K. N. *J. Am. Chem. Soc.* **2009**, *131*, 4084.
(25) For reviews, see: (a) van Zeist, W.-J.; Bickelhaupt, F. M. *Org. Biomol. Chem.* **2010**, *8*, 3118. (b) Fernández, I.; Bickelhaupt, F. M. *Chem. Soc. Rev.* **2014**, *43*, 4953. For recent examples of Diels−Alder reactions, see: (c) Kamber, D. N.; Nazarova, L. A.; Liang, Y.; Lopez, S. A.; Patterson, D. M.; Shih, H.-W.; Houk, K. N.; Prescher, J. A. *J. Am. Chem. Soc.* **2013**, *135*, 13680. (d) Liu, F.; Paton, R. S.; Kim, S.; Liang, Y.; Houk, K. N. *J. Am. Chem. Soc.* **2013**, *135*, 15642 and references cited therein.
(26) (a) Krenske, E. H.; Houk, K. N.; Holmes, A. B.; Thompson, J. *Tetrahedron Lett.* **2011**, *52*, 2181. (b) Krenske, E. H.; Davison, E. C.; Forbes, I. T.; Warner, J. A.; Smith, A. L.; Holmes, A. B.; Houk, K. N. *J. Am. Chem. Soc.* **2012**, *134*, 2434. (c) Krenske, E. H.; Perry, E. W.; Jerome, S. V.; Maimone, T. J.; Baran, P. S.; Houk, K. N. *Org. Lett.* **2012**, *14*, 3016. (d) Hong, X.; Liang, Y.; Brewer, M.; Houk, K. N. *Org. Lett.* **2014**, *16*, 4260.
(27) Vaughan, W. R.; Simonson, D. R. *J. Org. Chem.* **1973**, *38*, 566.

DOI: 10.1021/acs.joc.5b02288
J. Org. Chem. 2015, 80, 11039−11047